Accepted Manuscript

Algorithms for design optimization of chemistry of hard magnetic alloys using experimental data

Rajesh Jha, George S. Dulikravich, Nirupam Chakraborti, Min Fan, Justin Schwartz, Carl C. Koch, Marcelo J. Colaco, Carlo Poloni, Igor N. Egorov

PII: S0925-8388(16)31196-3

DOI: 10.1016/j.jallcom.2016.04.218

Reference: JALCOM 37416

To appear in: *Journal of Alloys and Compounds*

Received Date: 12 December 2015

Revised Date: 12 March 2016

Accepted Date: 21 April 2016

Please cite this article as: R. Jha, G.S. Dulikravich, N. Chakraborti, M. Fan, J. Schwartz, C.C. Koch, M.J. Colaco, C. Poloni, I.N. Egorov, Algorithms for design optimization of chemistry of hard magnetic alloys using experimental data, *Journal of Alloys and Compounds* (2016), doi: 10.1016/j.jallcom.2016.04.218.

Algorithms for design optimization of chemistry of hard magnetic alloys using experimental data

Rajesh Jha[a], George S. Dulikravich[a,*], Nirupam Chakraborti[b], Min Fan[c], Justin Schwartz[c], Carl C. Koch[c], Marcelo J. Colaco[d], Carlo Poloni[e], Igor N. Egorov[f]

[a]Florida International University, MAIDROC Laboratory, Department of Mechanical and Materials Engineering, 10555 West Flagler Street, Miami, Florida 33174, USA

E-mail of the corresponding author: dulikrav@fiu.edu

[b]Indian Institute of Technology, Department of Materials Engineering, Kharagpur, W.B.: 721302, India

[c]North Carolina State University, Materials Science and Engineering Department, Raleigh, NC 27695, USA

[d]Federal University of Rio de Janeiro/COPPE, Mechanical Engineering Department, Rio de Janeiro, Brazil

[e]University of Trieste, Dipartimento di Ingegneria e Architettura, Via Valerio, 10, 34127 Trieste, Italy

[f]SIGMA Technology, Electrozavodskaia St., 20, Moscow, 107023, Russia

Highlights

- Design of experiments algorithms created initial concentrations of alloying elements
- Multi-dimensional hyper-surfaces were used to fit experimental data
- Multi-objective optimization was used to find Pareto optimal concentrations
- Statistical measures determined the relative influence of individual elements

Abstract

A multi-dimensional random number generation algorithm was used to distribute chemical concentrations of each of the alloying elements in the candidate alloys as uniformly as possible while maintaining the prescribed bounds on the minimum and maximum allowable values for the concentration of each of the alloying elements. The generated candidate alloy compositions were then examined for phase equilibria and associated magnetic properties using a thermodynamic database in the desired temperature range. These initial candidate alloys were manufactured, synthesized and tested for desired properties. Then, the experimentally obtained values of the properties were fitted with a multi-dimensional response surface. The desired properties were treated as objectives and were extremized simultaneously by utilizing a multi-objective optimization algorithm that optimized the concentrations of each of the alloying elements. This task was also performed by another conceptually different response surface and optimization algorithm for double-checking the results. A few of the best predicted Pareto optimal alloy compositions were then manufactured, synthesized and tested to evaluate their macroscopic properties. Several of these Pareto optimized alloys outperformed most of the candidate alloys on most of the objectives. This proves the efficacy of the combined meta-modeling and experimental approach in design optimization of the alloys. A sensitivity analysis of each of the alloying elements was also performed to determine which of the alloying elements contributes the least to the desired macroscopic properties of the alloy. These elements can then be replaced with other candidate alloying elements such as not-so-rare earth elements.

Keywords

Design of alloys; Magnetic materials, Computational materials design; Response surfaces, Meta-models, Multi-objective optimization, Pareto-optimized predictions

1. Introduction

Rare Earth Element (REE) based magnets have a very high magnetic energy density ($(BH)_{max}$). This means that it is possible to synthesize smaller magnets while maintaining the superior magnetic properties. These magnets also have higher coercivity (H_c), making it difficult to demagnetize under external magnetic fields. Neodymium magnets are the strongest available magnets in this family. However, Nd-Fe-B (Neodymium-Iron-Boron) performs the best up to 150 ℃. From 150 ℃ to 350 ℃, Sm-Co (Samarium-Cobalt) magnets are used. These magnets usually need a protective coating in order to prevent corrosion. REE-based magnetic materials are essential in electric cars, in wind turbine electric generators, and any high-efficiency electric devices requiring magnetic fields. Hence, REEs are classified as strategic materials determining which national economies will survive and prosper in the post-combustion-engine era. Most of the REEs used for synthesizing these magnets are located in China and the Russian federation. Due to depleting resources and stringent trade rules from the suppliers, it is important to look at other options to synthesize these magnets [1].

AlNiCo magnets [2] are permanent magnetic alloys based on the Fe-Co-Ni-Al system without REEs. AlNiCo magnets have high B_r values, comparable to REE magnets. AlNiCo magnets have lower H_c values and can be demagnetized in the presence of an external magnetic field. A high B_r value can be properly exploited to cast this magnet in complex shapes, while magnetizing it in the production heat treatment stages. AlNiCo magnets possess excellent corrosion resistance and high-temperature stability. These are the only magnets that are stable up to 800 ℃ (Curie temperature). Above-

mentioned properties have been successfully exploited by researchers in the past and are a perfect choice for military and automotive sensor applications. Thus, any improvement in the existing properties of AlNiCo alloys will be helpful in covering the gap between the magnetic properties achieved by AlNiCo and REE based magnets.

In the present research work, a novel approach is presented for creating computational tools for design and multi-objective optimization of permanent magnetic alloys of AlNiCo type. This approach combines a number of numerical design optimization algorithms with several concepts from artificial intelligence and experimentally evaluated desired properties of an affordable set of candidate alloys. These alloys were further screened by various statistical tools in order to determine any specific trend in the data. This information will be helpful to the research community in developing a material knowledge base for the design of new alloys for targeted properties.

At present, researchers around the globe are working on designing magnetic alloys that will be able to cover the gap between the properties achieved by AlNiCo magnets and the rare-earth magnets, basically by adding a small amount of those rare-earth elements that are less critical in the sense of supply [3,4]. Sellmyer et al. [5] worked on a few rare-earth free alloys. Zhou et al. [6] manufactured a few commercial AlNiCo alloys to demonstrate the scope of improvement in this field. The difference between the theoretically calculated and the experimentally measured properties was quite large for both ($(BH)_{max}$) and H_c. Thus, random experimentation may prove to be both expensive and time-consuming.

Designing a new alloy system is a challenging task mainly due to a limited experimental database. In order to develop a reliable knowledge base [7] for design of new alloys, one needs to focus on determining various correlations (composition-property, property-

property, and composition-composition) from the available databases (simulated and experimental). This information can be coupled with the theoretical knowledge (atomistic and continuum based theories) to develop the knowledge base. Integrated Computational Materials Engineering (ICME) approach [8] and materials genome initiative highlighted the importance and growing application of computational tools in the design of new alloys. In recent years, various data-driven techniques combined with evolutionary approaches [9] have been successfully implemented in direct alloy design [9-14] and inverse alloy design [15] and in improving thermodynamic databases such as Thermocalc [16] for alloy development. Jha et al. [12,13] demonstrated the scope of use of these databases for designing Ni-based superalloy and Rettig et al. [14] performed a few experiments to confirm his findings. Data mining approaches such as Principal Component Analysis (PCA) and Partial Least Square (PLS) regression have been successfully used in designing new alloys [17,18]. Additionally, various machine-learning algorithms have been used to address a vast range of problems in materials design [19,20].These applications demonstrate the efficacy of application of computational tools for materials design.

Mishima in Japan [2] first discovered AlNiCo magnets in 1931. Initially, it belonged to the Fe-Co-Ni-Al quaternary system. Magnetic properties in these magnets were attributed to shape anisotropy in the two-phase system, the phases being rod like Fe-Co rich ferromagnetic phase α_1 and Ni-Al rich phase α_2 (Body Centered Cubic (BCC)). It was later observed that shape anisotropy is a result of a metallurgical phenomenon popularly known as spinodal decomposition in the temperature range of 800-850 ºC. Shape anisotropy results in periodic distribution of phase α_1 in the matrix of α_2 phase. The axis of elongation of α_1 rods are parallel to <100> direction. Phases α_1 and α_2 are stable up to 850 ºC, that is, just below the Curie temperature, which is about 860 ºC for

AlNiCo alloys. Above 850 ºC, Face Centered Cubic (FCC) γ phase begins to appear and it was observed in a few samples [21]. Gamma phase must be avoided, as it is detrimental for magnetic properties. Various attempts (such as modification of heat treatment protocol and addition of various alloying elements) have been made to stabilize the magnetic α_1 and α_2 phases and simultaneously eliminate or reduce the amount of γ phase. In the past few decades, (especially after the discovery of powerful REE-based magnets in 1980's), there has been limited research on AlNiCo magnets. Recent rise in prices of rare earth elements led to the search for rare-earth free magnets. In recent years, AlNiCo magnets are again a popular choice for research mainly due to their proven high-temperature stability and related properties at an affordable cost [22].

Currently, AlNiCo alloys are not limited to quaternary systems and may contain eight or more elements [2,10,11,13,23]. In this work, we selected eight elements namely Iron (Fe), Cobalt (Co), Nickel (Ni), Aluminum (Al), Titanium (Ti), Hafnium (Hf), Copper (Cu) and Niobium (Nb). Variable bounds of these elements have been tabulated in Table 1. From both experimental as well as the modeling point of view, it will be helpful to discuss the role of these alloying elements. This information can be utilized to select meta-model for targeted properties. This will be helpful in developing a knowledge base for discovery of new materials and/or improving properties of existing materials.

As shown in Figure 1, magnetic energy density ($(BH)_{max}$) is defined as the area of the largest rectangle that can be inscribed in the second quadrant of B-H normal curve [24]. Since, H_c and B_r are conflicting; one has to sacrifice on one of these properties to improve the other property. Therefore, in order to increase $(BH)_{max}$, one needs to optimize H_c and B_r.

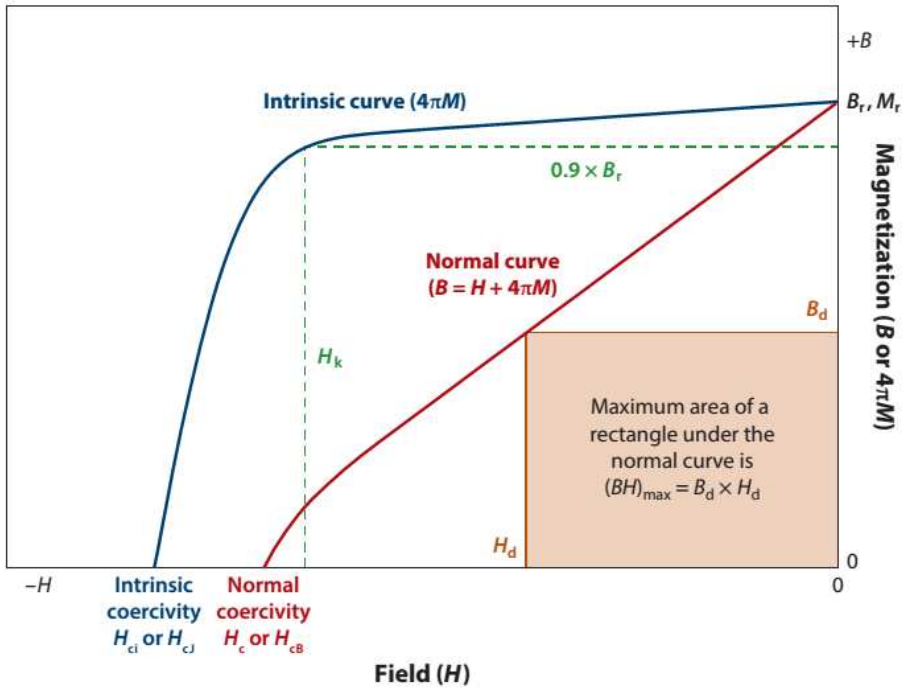

Fig. 1

B-H curve: shows relation between Hc, Br and ((BH)max) [24].

The following text will provide the reader with a brief idea regarding the role of various alloying elements and its effect on H_c and B_r [21]:

Cobalt: It is a γ stabilizer. A solutionization anneal is needed to homogenize it to a single α phase. Cobalt increases coercivity and Curie temperature.

Nickel: It is also a γ stabilizer. Hence, solutionization anneal temperature needs to be increased in order to homogenize it to a single α phase. Nickel increases Hc (less than Cobalt) while decreases Br.

Aluminum: It is an α stabilizer. It will be helpful in reducing the solutionization anneal temperature. Aluminum is expected to affect Hc positively.

Copper: It is an α stabilizer. Research shows that Copper affects Hc and Br positively and increases it. In AlNiCo 8 and AlNiCo 9 alloys, Cu precipitates out of the α2 phases into particles and is responsible for the magnetic separation between α1 and α2 phases. An increase in phase separation leads to an increase in Hc.

Titanium: It is an α stabilizer and one of the most reactive elements. It reacts with impurities such as C, S, and N and purifies the magnet by forming precipitates with these elements. It helps in grain refining but it is detrimental for columnar grain growth. S and Te additions can help in regaining grain growth capabilities. Majority of grains are aligned perpendicular to the chill plate due to columnar grain growth and large shape anisotropy can be achieved if spinodal decomposition occurs in this direction. Titanium increases Hc at the expense of Br [25].

Niobium: It is an α stabilizer. It forms precipitate with Carbon. Carbon is a strong γ stabilizer and needs to be eliminated. Like Ti, Nb also inhibits columnar grain growth. Nb increases Hc, at the expense of Br [26].

Hafnium: It is used for enhancing high-temperature properties. It precipitates at the grain boundary and helps in improving creep properties. Recent studies related to Co-Hf magnets [5], motivated us to use Hf in this work.

From the above literature, the reader can understand the role that spinodal refining plays in improvement of properties of these magnets. Several research groups have developed their theories for improved properties of these magnets. $(BH)_{max}$ is dependent on both Br and Hc and it is proportional to Hc at low Hc. For example, a recent study on nanostructured magnetic material suggests that it is possible to achieve a very high magnetic energy product for fine wires of the order of 10 nm [21]. Directionally aligned rods obtained because of shape anisotropy due to spinodal

decomposition in AlNiCo alloys were approximated as such fine wires. As per this theory, the upper bound of (BH)max was theoretically calculated and was found to be an order of magnitude greater than the best commercially available AlNiCo alloy. According to this theory, (BH)max is directly proportional to Mr (remanence magnetization), while Mr is directly proportional to Ms (saturation magnetization). Thus, the lower bound of (BH)max is proportional to Hc, and the upper bound of (BH)max has been reported to be proportional to Ms.

It must be noted that Hc is an extrinsic property, while Ms is an intrinsic property of the magnet. Thus, experimentalists have to be extremely careful while preparing specimens and designing thermomagnetic treatment protocols. They also must have access to advanced diagnostic tools required for analysis at nanometer scale.

Two recent papers [6, 22] reported the importance of copper rich precipitates between adjacent α_1 phases and their importance in improvement of magnetic properties for AlNiCo 8 and 9 grade alloys.

2. Algorithms for multi-objective design optimization of alloys

We used a set of computational tools to develop a novel approach for design and optimization of high-temperature, high-intensity magnetic alloys. The steps involved in the proposed approach can be listed as follows:

1. Initial dataset: From our own expertise and the open literature, we defined the variable bounds of eight alloying elements that are to be used for the manufacture of magnets. One of the best-known quasi-random number generators, Sobol's algorithm [27], was used to generate chemical concentrations for an initial set of 80 candidate alloys (Table 1 and Table 2). These alloys were screened on the basis of limited knowledge of phase

equilibrium and magnetic properties from a commercial thermodynamic database, Factsage [28].

2. Manufacture and testing: These alloys were synthesized and tested for various properties of interest as shown in Table 3. A summary of the manufacture and testing protocol in listed here with more information presented in [29, 30].

    a. Manufacture: Bulk samples were cast in a water cooled copper hearth. The specimens were re-melted at least three times to ensure homogenization.

    b. Thermo-magnetic treatment: Cast samples were solutionized at 1250 ^{0}C and then thermo-magnetically treated at 800 ^{0}C for 10 minutes. Magnetic field (3T) was applied in the direction of cylindrical axis.

    c. Hysteresis measurements: They were performed by Quantum Design superconducting quantum interference device (SQUID) magnetometer, where magnetic field varied between -3T to +3T at room temperature. Br, Hc and (BH)max were obtained from hysteresis loops obtained in this step.

    d. Structural and compositional properties were analyzed by:

        i. Transmission electron microscope (TEM).

        ii. Energy-dispersive x-ray spectroscopy (EDS) analysis.

3. Response surface generation: This data was used to link alloy composition to desired properties by developing response surfaces for those specific properties (listed in Table 3). A commercial optimization package, modeFRONTIER [31] was used for this purpose. Response surfaces were

tested on various accuracy measures and the most accurate one was chosen for further study. Various approaches were used to develop response surfaces. These include Radial basis functions (RBF), Kriging, Anisotropic Kriging, and Evolutionary Design.

4. Multi-objective optimization: Response surfaces selected above were used to extremize various properties as per the objectives specified in Table 3. It was observed that most of the optimization tasks yielded alloys with a similar chemical composition for a set of objectives. Hence, several optimization runs were performed to get a diverse pool of results. Various optimization algorithms were used for this purpose. It includes Non-dominated Sorting Genetic Algorithm II (NSGA2), Multi-Objective Particle Swarm Optimization (MOPSO), Multi-Objective Simulated Annealing (MOSA) and FAST optimizer which uses response surface models (meta-models) to speed up the optimization process using search algorithms such as NSGA2, MOPSO, MOSA [31].

For the purpose of self-evaluation, this work was independently carried out at three different places using:

a. Commercial optimization package, Indirect Optimization based on Self-Organization (IOSO) algorithm [9].
b. Hybrid response surface [32] was used because of its robustness, accuracy and computational efficiency. Multi-objective optimization was performed by Non-Dominated Sorting Genetic Algorithm (NSGA2) [31].
c. Surrogate model selection algorithm [32] was used because of its robustness and simplicity.

Pareto-optimized predictions from the above optimization packages were merged. From this set, we selected a few alloys for further manufacture and testing.

5. The work has been performed in cycles. Steps 2-5 were repeated until the improvements of multiple macroscopic properties of these magnetic alloys became negligible.

6. Sensitivity analysis: Various statistical tools were used to determine composition-property relations. This was done in order to find influential alloying elements for development of knowledge base. At the same time, the sensitivity analysis also helps in finding the least influential alloying elements that could be discarded to make way for introduction of affordable and readily available rare-earth elements.

This work will help in developing a knowledge base that will be useful to the research community in designing new alloys. In data-driven material science, knowledge discovery [7] for designing new materials requires:

a) Data: In this work, our database is a combination of experimentally verified data and Pareto-optimized predictions.

b) Correlations: Various linear and nonlinear correlation, clustering, and a principal component analysis tool to discover various trends in the dataset.

c) Theory: The above information can be coupled with theoretical knowledge to motivate the experimentalist to modifying standard manufacturer protocol for the design of new alloys.

Table 1: Concentration bounds used for optimization of AlNiCo type alloys

Alloys number	1-85	86-143	144-173
Alloying elements	Concentration bounds (wt. percent)		
Cobalt(Co)	24 - 40	24 - 38	22.8 - 39.9
Nickel (Ni)	13 - 15	13 - 15	12.35 - 15.75
Aluminum (Al)	7 - 9	7 - 12	6.65 - 12.6
Titanium (Ti)	0.1 - 8	4 - 11	3.8 - 11.55
Hafnium (Hf)	0.1 - 8	0.1 - 3	0.095 - 3.15
Copper (Cu)	0 - 6	0 - 3	0.4 - 5
Niobium (Nb)	0 - 2	0 - 1	0 - 1.5
Iron (Fe)	Balance to 100 percent		

Table 2: Cycle and alloy number

Cycle number	Number of alloys designed	Best alloy
1	1-80	#30
2	81-85	#84
3	86-90	#86
4	91-110	#95
5	111-120	#117
6	120-138	#124
7	139-143	#139
8	144-150	#150
9	150-160	#157
10	160-165	#162

11	166-173	#169

Table 3: Quantities to be simultaneously extremized using multi-objective optimization

	Properties	Units	Objective
1	Magnetic energy density ($(BH)_{max}$)	kg m^{-1} s^{-2}	Maximize
2	Magnetic coercivity (H_c)	Oersted	Maximize
3	Magnetic remanence (B_r)	Tesla	Maximize
4	Saturation magnetization (M_s)	Emu/g	Maximize
5	Remanence magnetization (M_r)	Emu/g	Maximize
6	$(BH)_{max}$/mass	m^{-1} s^{-2}	Maximize
7	Magnetic permeability (μ)	kg m A^{-2} s^{-2}	Maximize
8	Cost of raw material (cost)	$/kg	Minimize
9	Intrinsic coercive field (jH_c)	A m^{-1}	Maximize
10	Density(ρ)	Kg m^{-3}	Minimize

3. Results

As discussed in Section 2, we have worked through 11 cycles of design and optimization, each of them including its own experimental validation. Table 2 lists the Pareto-optimized alloys manufactured in each of the design cycles and the best experimentally validated alloy in each cycle.

Work done in all the cycles is described as follows:

1. Cycle 1 (Alloys 1-80): Initial alloy compositions were predicted by Sobol's algorithm [27] and the initial set of 80 elements was chosen for manufacture

and testing. Thereafter, we proceeded further with design and optimization with the goal of improved results.

2. Cycle 2 (Alloys 81-85): One of the predicted alloys (alloy 84) outperformed the initial set of alloys as well as the other Pareto-optimized predictions. This demonstrates the efficacy of the current approach and we moved forward with the objective of further improvements. The variable bounds were updated (for alloy 86-90) and listed in Table 1.

3. Cycle 3 (Alloys 86-90): Alloy 86 was the best candidate in this set. Measured properties of the new set (alloy 86-90) were in the vicinity of the previous pool of alloys. One of the reasons for this can be non-uniform distribution of alloying elements in the variable space. Since there was no significant improvement; the next set of alloys was predicted by Sobol's algorithm so as to provide additional support points in the variable space for development of response surfaces with improved accuracy.

4. Cycle 4 (Alloys 91-110): Alloy 95 was the best performer in this group. Our approach of providing more support points for the response surfaces proved helpful in the improvement of properties. Alloy 95 had an H_c of 980 Oe (against 750 Oe for the previous best alloy 84).

5. Cycle 5 (Alloys 111-120): Alloy 117 is the best alloy in this dataset in terms of ((BH)max). There was a significant improvement in the properties of the new alloys. Alloy 111 and 114 had an H_c of 1050 Oe while alloy 117 reported 1000 Oe (against 980 Oe for the previous best alloy 95). This improvement motivated us to proceed towards the next cycle of design and optimization task.

6. Cycle 6 (Alloys 121-138): Alloy 124 was the best performer in this group. There was a significant improvement in both ($(BH)_{max}$) and H_c. Hence, we moved forward towards the next cycle of design and optimization.

7. Cycle 7 (Alloys 139-143): Alloy 139 was the best performer in this group. Its properties were in the vicinity of alloy 124. Since, there was no significant improvement in the desired properties, the design and optimization process was halted in order to minimize waste of resources and funding. The created a need to perform a sensitivity analysis of the variables and associated properties.

Cycles 8-11 (Alloys 144-173): In these cycles, variable bounds were relaxed by 5 percent, while the methodology remained the same.

8. Cycle 8 (Alloys 144-150): Alloys predicted by modeFRONTIER. Marginal improvement in H_c was observed, but there was no significant improvement in other properties.

9. Cycle 9 (Alloys 151-160): Alloys predicted by Surrogate model selection algorithm(SM). There was no significant improvement in any of the properties.

10. Cycle 10 (Alloys 161-165): Alloys predicted by modeFRONTIER. Marginal improvement in H_c was observed, however, there was no significant improvement in other properties.

11. Cycle 11 (Alloys 166-173): Alloys predicted by hybrid response surface and modeFRONTIER. Marginal improvement in H_c was observed, but there was still no significant improvement in other properties.

Figures 2, 3 and 4 show the comparison between various approaches for a set of properties. It can be observed that the alloys predicted by meta-modeling and optimization dominate the ones predicted by Sobol's algorithm [27]. One can observe significant improvement over the cycles. Experimentally verified H_c values are at par with commercial alloys [6]. We expect improvement in $(BH)_{max}$ and B_r values in the next few cycles. At this point, we have a significant amount of experimentally verified data. Hence, we felt the need to perform a sensitivity analysis of the response surfaces and look for patterns in the dataset.

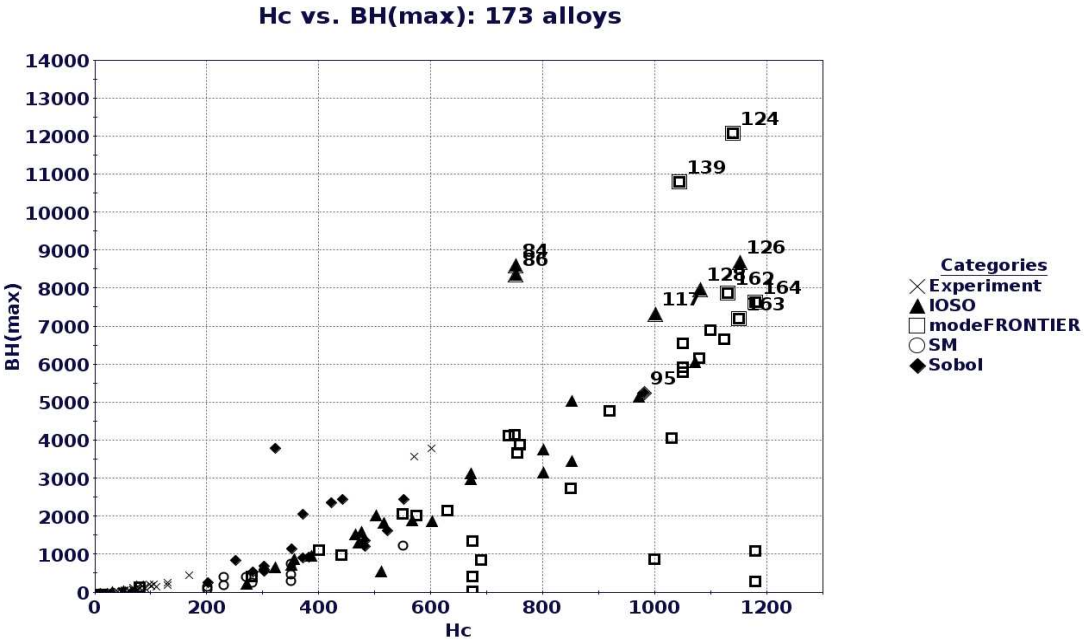

Fig. 2.

Magnetic energy density *vs*. magnetic coercivity; comparison of solutions by various approaches

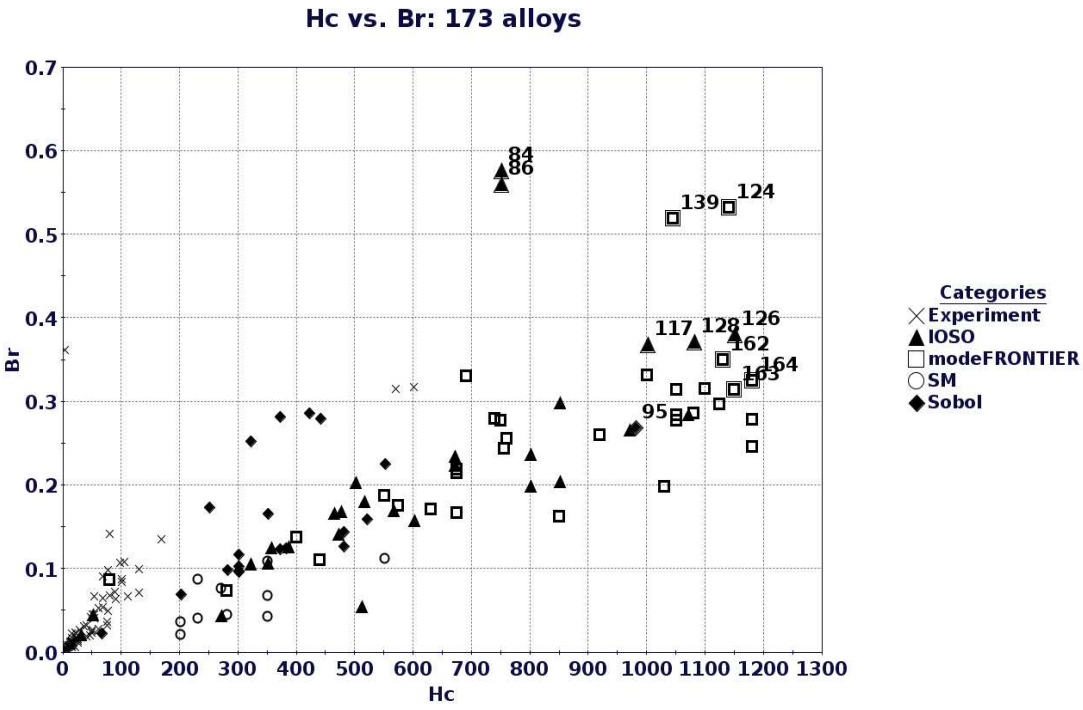

Fig. 3.

Magnetic coercivity *vs.* magnetic remanence, comparison of solutions by various approaches

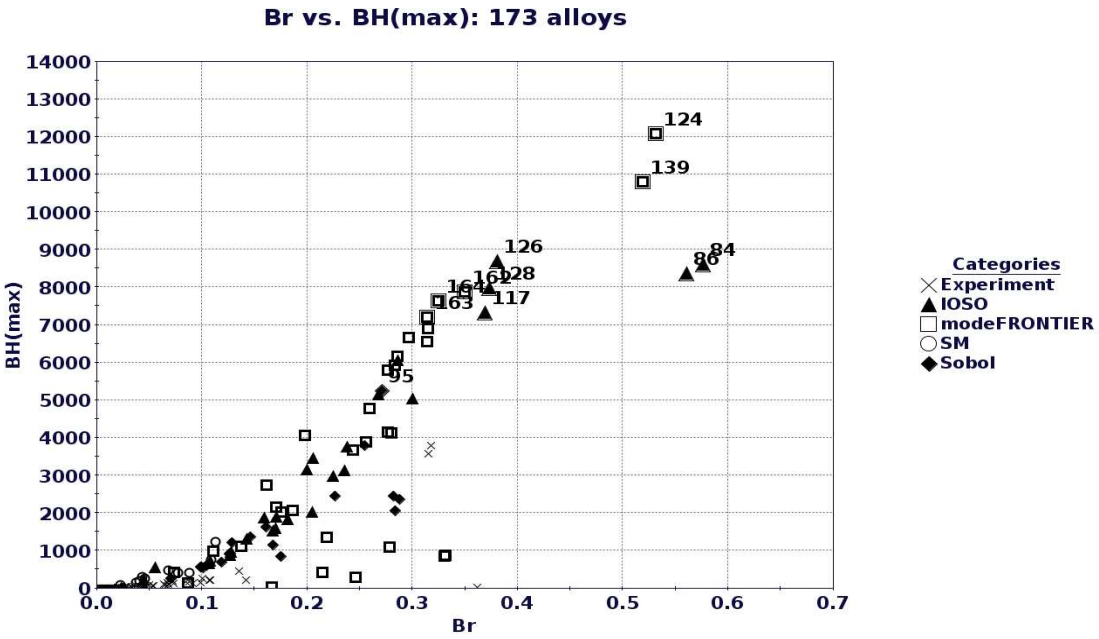

Fig. 4.

Magnetic energy density *vs.* magnetic remanence, comparison of solutions by various approaches

4. Sensitivity analysis

It was done in order to determine the composition-property relationship. Another purpose was to find various trends and patterns within the dataset. Initially, Pearson's linear correlation method was used. It was followed by various approaches to determining non-linear trends within a dataset [19].

Single Variable Response (SVR)

This is a methodology that is often applied for qualitative analysis of the training results obtained from Evolutionary Neural Network [34] and Bi-Objective Genetic Programming [35,12]. In SVR, a trend is created by generating values between zero and one on a time scale. The trend line is irregular. Specifically, there are regions of constant values,

sharp increases, and sharp decreases in the line. This has been referred to as an input signal in the following text. For SVR testing, the input signal (a trend of variation) was used for one of the variables while the other variables were kept constant at an average value. The various responses were tabulated in Table 4 for each of the models. For the responses, the following terminologies were used:

Dir: This means that the model output increases by increasing the value of an input signal and decreases on decreasing the input value.

Inv: This means that a particular variable increase will cause the property value to decrease and *vice versa*.

Nil: This means that the model was unable to find any correlation between that particular variable and the model output.

Mix: This means that the model has a different response for a different set of data of any particular variable.

Since, the dataset is quite noisy, the responses were mixed (Table 4). However, a few important findings can be listed as follows:

1) Copper shows a direct response for H_c and B_r. Thus, response surface predictions are of comparable accuracy with available results in the open literature as discussed in Section 2.1.
2) Hafnium shows a direct response for $H_c$and B_r. Further experiments/ data analysis are needed before reaching a conclusion regarding the effect of Hf on H_c and B_r as it has not been previously used in AlNiCo alloys.
3) Nickel shows response for $(BH)_{max}$.

These findings are promising as they mimic the findings from the literature. Hence, meta-modeling can prove to be an asset for developing alloys in the future. In order to proceed further, we need to evaluate our findings by other data-mining techniques.

Table 4: Single variable response (SVR) for various macroscopic properties of AlNiCo type alloys

Objective No.	Properties	Variable response							
		Fe	Co	Ni	Al	Ti	Hf	Cu	Nb
1	Magnetic energy density ((BH)max)	Nil	Nil	Mix	Nil	Nil	Nil	Nil	Nil
2	Magnetic coercivity (Hc)	Mix	Mix	Mix	Inv	Mix	Dir	Dir	Mix
3	Magnetic remanence (Br)	Mix	Mix	Mix	Inv	Mix	Dir	Dir	Inv
4	Saturation magnetization (Ms)	Dir	Inv	Dir	Mix	Inv	Dir	Mix	Mix
5	Remanence magnetization (Mr)	Nil	Nil	Nil	Nil	Nil	Nil	Nil	Nil
6	(BH)max/mass	Nil	Nil	Nil	Nil	Nil	Nil	Nil	Nil
7	Magnetic permeability (μ)	Mix	Mix	Mix	Mix	Inv	Mix	Mix	Mix
8	Cost of raw material (cost)	Inv	Inv	Inv	Dir	Dir	Dir	Inv	Dir

9	Intrinsic coercive field (jHc)	Mix	Mix	Mix	Inv	Inv	Mix	Dir	Mix
10	Density(ρ)	Mix	Dir	Mix	Inv	Inv	Mix	Mix	Dir

Principal Component Analysis (PCA)

Principal component analysis can be classified as an unsupervised learning machine-learning algorithm [19,20]. It was performed in order to determine correlations between variables and various properties by reducing the dimensionality of the dataset without losing much information. PCA uses an orthogonal transformation to convert a set of usually correlated variables (or properties) into a set of values of linearly uncorrelated variables known as Principal Components (PCs). Hence, each PC is a linear combination of all the original descriptors (variables and properties). The first principal component (PC1) accounts for maximum variance in the dataset, followed by PC2 and so on [7,31]. Thus, it is possible to visualize a high dimensional dataset by choosing first two or three PCs [19,20]. It is also used for identifying patterns in data, as patterns may be hard to find in high-dimensional data sets.

PCA was conducted separately for design variables (alloying elements) and targeted properties. For design variables, all the eight elements were included for PCA. We have 8 design variables (alloying elements), thus there will be maximum of 8 PCs.

For targeted properties, it can be observed that apart from $(BH)_{max}$/mass, all other properties were measured independently. $(BH)_{max}$/mass was, thus, removed from further analysis to reduce the complexity of the problem. We were left with 9 targeted properties. Hence, there was a maximum of 9 PCs. Prior to PCA, three important terms need to be discussed for better understanding of the analysis results:

a) Scree plot: It is a plot between Eigen values and component number. It is an important parameter used to select the number of components required to represent the complete dataset. Usually, components with eigen values above one (1) are chosen for further analysis. It can be seen from the figures in the later part that the scree plot usually flattens below eigenvalue 1. This means that the later components do not have any significant effect on the dataset. Since each successive component accounts for comparatively less variance, the least influential components can be ignored from further analysis.

b) Eigen values: are the variances of the principal components. PCA was conducted on the correlation matrix. Here, the variables were standardized, so that each variable has a variance of one, and the total variance is equal to the number of variables used in the analysis. Thus, there will be eight PCs for elements and nine PCs for properties. The first component will always account for the most variance (and hence will have the highest eigenvalue). Next, components will account for as much of the left over variance as they can. Hence, each successive component will account for comparatively less variance (hence less eigenvalues) than the one preceding it.

c) Component plot: After the required number of components are chosen, these components are plotted against each other, while the original variables (or properties) are plotted on this reduced space. Orientation of a certain variable (or property) on the reduced space determines its contribution towards a certain PC. That is, if the variable is positioned along PC1 on the 0-line perpendicular to PC2, this variable will have maximum influence on PC1 and minimum influence

on PC2. This will be better explained with the corresponding figures in the latter part of the text.

In Figure 19 and 20, alloys were also plotted along with the elements. Here, the alloys are clustered by K-means clustering method to classify the alloys into different clusters. Alloys that belong to the same cluster have the same symbol. A few of the best alloys mentioned in Table 2 are plotted on the figure. In these figures, variables (elements) are plotted as arrows. Arrows represent the relative contribution of the original variables to the variability along the PCs. In these figures, the longer the arrows, the stronger are their contributions. Additionally, an arrow orthogonal to a certain PC has null effect on that PC while an arrow that is collinear to a certain PC contribute only to that certain PC.

We classified the dataset into four sets and performed the PC analysis on individual sets in order to extract information from one set and then cross-check it with the findings of other sets. In all of these cases, PC1, PC2, and PC3 were able to capture most of the variance of the dataset. Dataset was classified as follows:

a) Experimental: Alloy #1-80

b) Optimization: Alloy # 81-173

c) Data categorized based on Multi-Criterion Decision Making (MCDM): 40 alloys were selected.

d) Whole dataset: Alloy # 1-173.

We used a popular statistical software, IBM SPSS [36], and Multivariate Data Analysis (MVA) node in optimization package modeFRONTIER [31] for this work.

a) Experimental: Alloys 1-80

These 80 alloys represent the initial set of compositions predicted by Sobol's algorithm [27]. Hence, we did not perform PCA on the elements. Various properties were analyzed and reported below. Scree plots were created in order to determine the number of effective principal components required to represent the whole dataset. It was found that two PCs are able to extract most of the information from the dataset. Figure 5 shows the scree plot for the properties, while Figure 6 shows the orientation of various properties in the PC space.

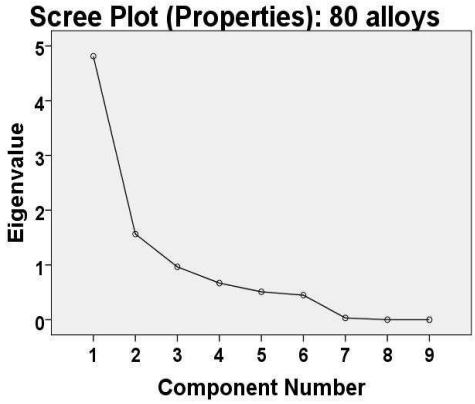

Fig. 5.
Scree plot for PC analysis: Two PC components were chosen

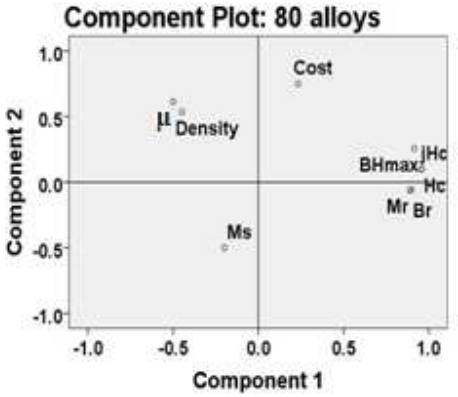

Fig. 6.
Orientation of various properties in the PCA space

Figure 6 shows that $(BH)_{max}$, jH_c, H_c, M_r and B_r have maximum effect on PC1 while cost and M_s has maximum effect on PC2. Density and μ have similar effects on both PC. It can be seen that H_c and jH_c coincide at the same spot thus H_c and jH_c seems to be dependent on each other. It makes sense, as one is the inverse of the other. Similarly, M_r and B_r can be clustered together and μ and density can be taken as another cluster. This means that properties that form a cluster may affect, or may be dependent on, each other. Analysis of other datasets will further clarify these findings.

b) Optimization: Alloys 81-173

In this data, we went for PC analysis for the elements. From scree plot in Figure 7, it was found that three PCs are able to extract most of the information from the dataset. Figure 7 shows the scree plot for the elements while Figure 8 shows the position of various elements in the PC space.

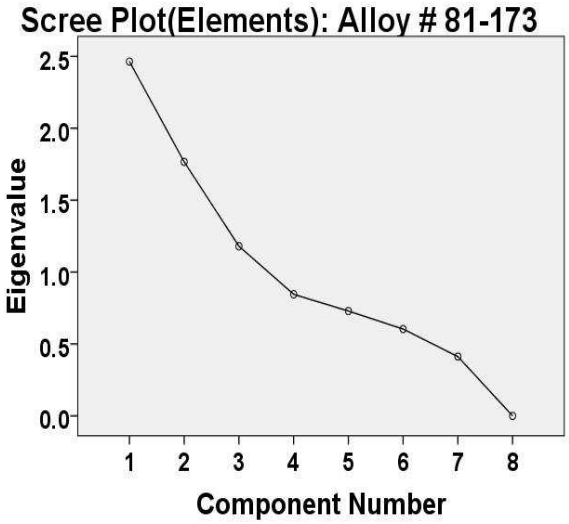

Figure 7: Scree plot for PC analysis: Three PC components were chosen

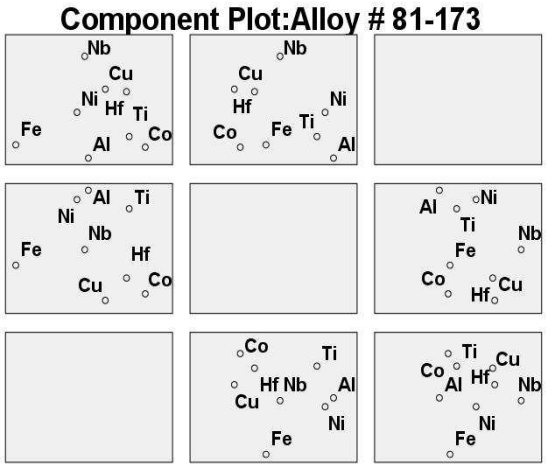

Figure 8: Orientation of various elements in the PC space

In Figure 8, one can observe that elements have mixed effect on the three selected PCs. Since various optimizers and Sobol's algorithm have predicted these alloys composition, it seems to be properly distributed in the variable space. Hence, such a relation can be expected.

Upon close observation, it can be seen that Cu and Hf are close enough to form a cluster. This means that Cu and Hf may affect the properties of the alloy in a similar way. From SVR analysis, both Cu and Hf showed a direct response for H_c and B_r. Hf usually precipitates at the grain boundaries and enhances high temperature properties.

However, it has been rarely used in AlNiCo alloys; hence, this finding can be helpful for the experimentalist to proceed forward for Hf addition in AlNiCo alloys. This must be analyzed further in other datasets before moving for microstructure analysis. Ni and Al can also be clustered together and appear to have similar effect. This can be supported from the literature, as there exists Ni-Al rich phase in these alloys.

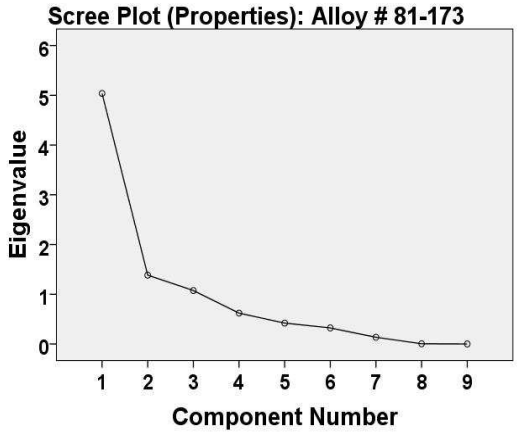

Fig. 9.

Scree plot for PC analysis: Three PC components were chosen

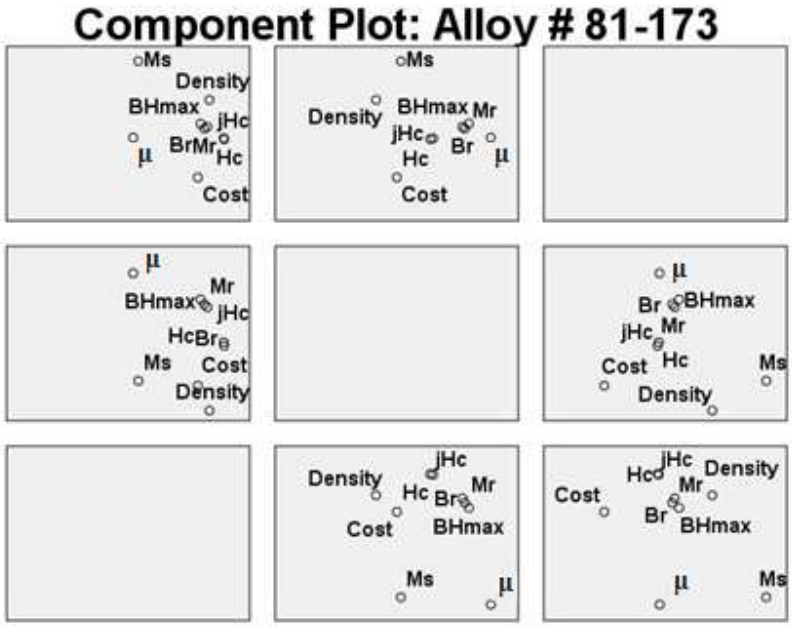

Fig. 10.

Orientation of various properties in the PC space

It was found that three PCs are able to extract most of the information from the dataset. Figure 9 shows the scree plot for the elements, while Figure 10 shows the position of various properties in the PC space. In Figure 10, H_c and jH_c are clustered together. It can be seen that B_r, M_r, and $(BH)_{max}$ can be clustered as well. B_r and M_r were clustered in the previous analysis. Hence, these properties may be correlated (or dependent) on each other.

c) Data categorized based on Multi-Criterion Decision Making (MCDM): 40 alloys were selected

Due to software limitations, we focused on optimizing $(BH)_{max}$, H_c and B_r only. We left the other properties of interest though they are quite important for the magnet. In this

part, we selected 40 alloys based on objectives defined in Table 2. We used Multi-Criterion Decision Making methodology to select these alloys.

Based on eigen values, three PCs were chosen (Figure 11). Figure 12 shows the orientation of various elements on the PC space. Figure 12 supports our finding from the previous set regarding Cu and Hf. In this set too, Cu and Hf can be clustered together. Similarly, Ni and Al can be clustered together.

Figure 13 shows scree plot for various properties while Figure 14 shows the orientation of these properties in the PC space. In Figure 14, Mr and Br can be clustered and hence these properties may be dependent on each other. $(BH)_{max}$ does not seem to be part of the cluster anymore, but is close to it. Finally, we can proceed towards analyzing the whole dataset.

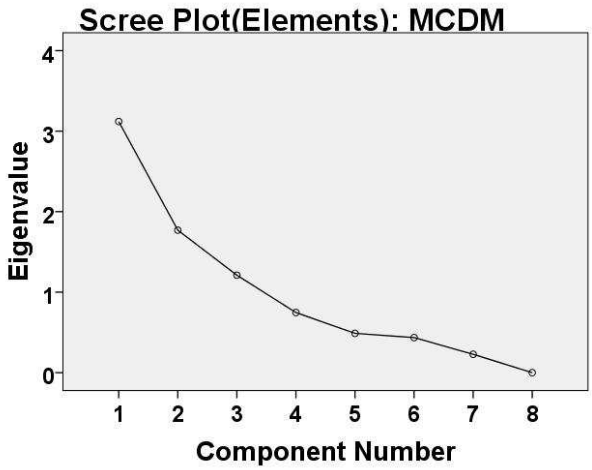

Fig. 11.

Scree plot for PC analysis: Three PC components were chosen

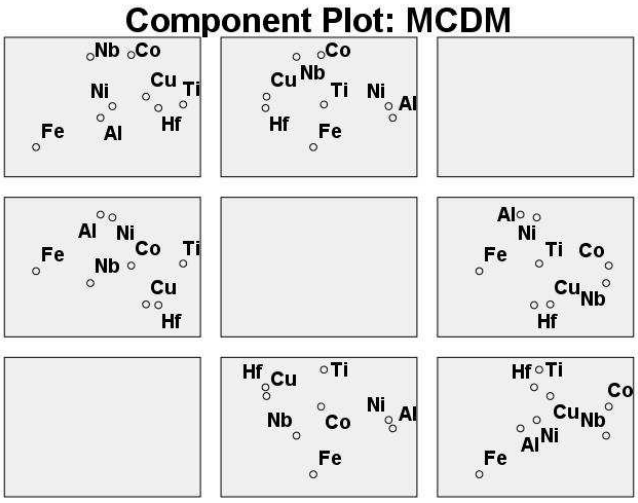

Fig. 12.

Orientation of various elements in the PC space

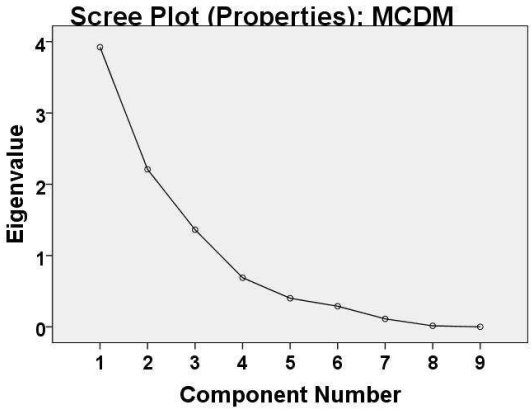

Fig. 13.

Scree plot for PC analysis: Three PC components were chosen

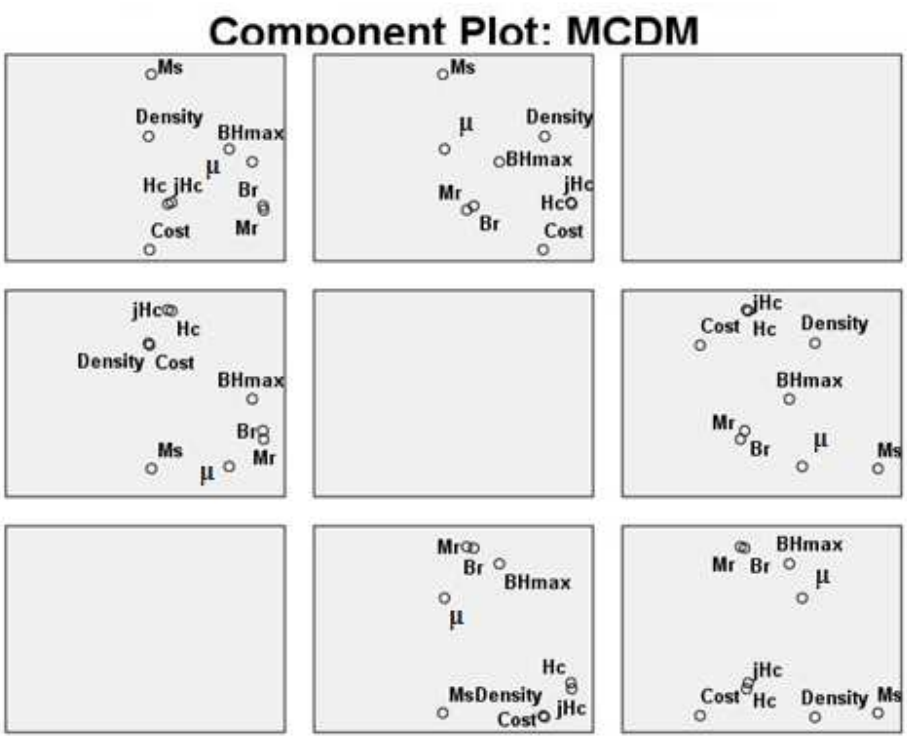

Fig. 14.

Orientation of various properties in the PC space

c) Whole dataset: Alloys 1-173.

Here, the complete dataset was used for analysis. Figure 15 shows the plot for various elements. Based on eigen values, three PCs are able to extract most of the information from the dataset.

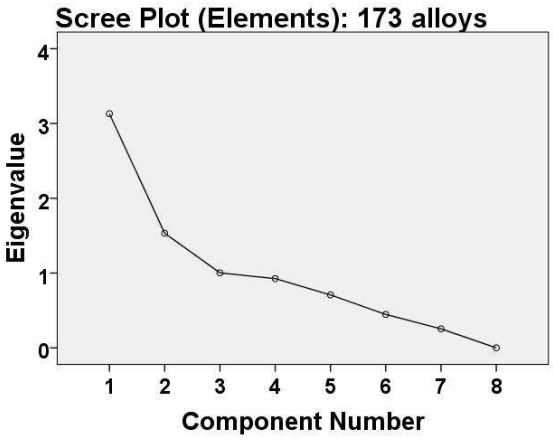

Fig. 15.

Scree plot for PC analysis: Three PC components were chosen

Figure 16 shows the orientation of various elements in the PC space. Cu and Hf can be clustered together (Figure 16). In PC1 *vs.* PC2 (top corner), Ti can also be clustered along with Cu and Hf. Ni and Al can be clustered together. Hence, we have sufficient information from the above analysis to move forward towards microstructure analysis.

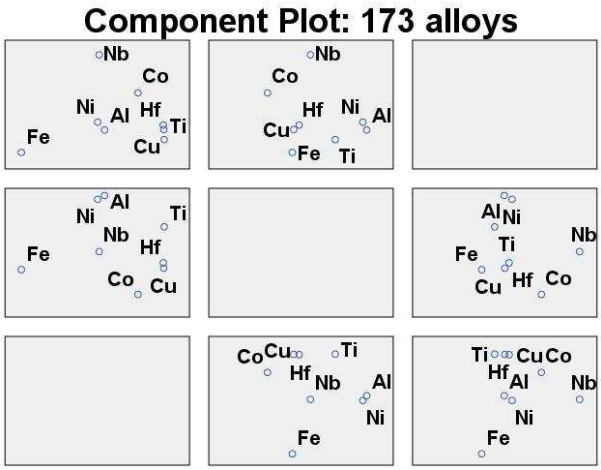

Fig. 16.

Orientation of various elements in the PC space

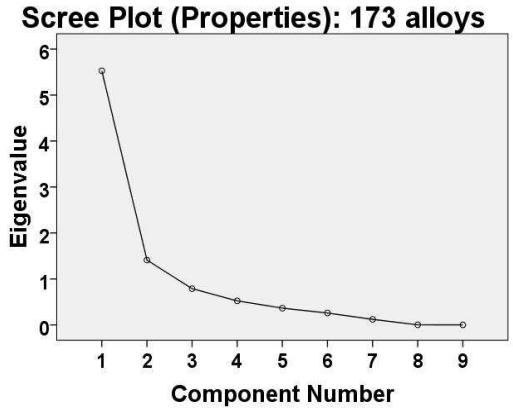

Fig. 17.

Scree plot for PC analysis: Two PC components were chosen

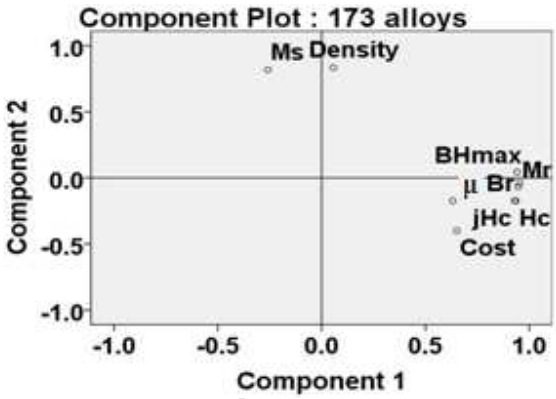

Fig. 18.

Orientation of various properties in the PC space

Figure 17 shows the scree plot for various properties. Based on eigen values, two PC's can extract most of the information from the dataset. Figure 18 shows the orientation of various elements in the PC space. In Figure 18, it can be observed that $(BH)_{max}$, B_r, μ, H_c, jH_c and M_r contributes strongly on PC1, while Ms and density strongly contributes towards PC2. $(BH)_{max}$, B_r, and M_r can be clustered together. These findings are in line with the previous observations. Hence, we can proceed further and look towards the orientation of various alloys on the PC space along with the alloying elements. Here, the alloys were plotted on the PC space along with the elements. Here, the element's contribution towards a certain PC is related to the length and orientation of the arrow corresponding to that particular PC. Cluster analysis was performed by K-means clustering (Kaufman approach). Davies-Bouldin index (D-B index), is a measure of quality of clustering and it is used for determining the appropriate number of clusters

into which the dataset can be divided. D-B index is the sum ratio of internal variance of each cluster with inter-cluster distance. In partitive clustering, one prefers small internal variance of each cluster along with high inter-cluster distances. Thus, D-B- index needs to be minimized. That is, number of clusters corresponding to lowest D-B index is applied on the dataset. Based on D-B index, the data set was divided into 8 clusters. Alloys belonging to different clusters were denoted by different symbols in Fig. 19 which used 173 alloys that were actually manufactured and experimentally evaluated. A few alloys were marked in order to avoid overlapping and give clear understanding. These alloys are from the best alloys ranked based on $(BH)_{max}$ values (as mentioned in Table 2).

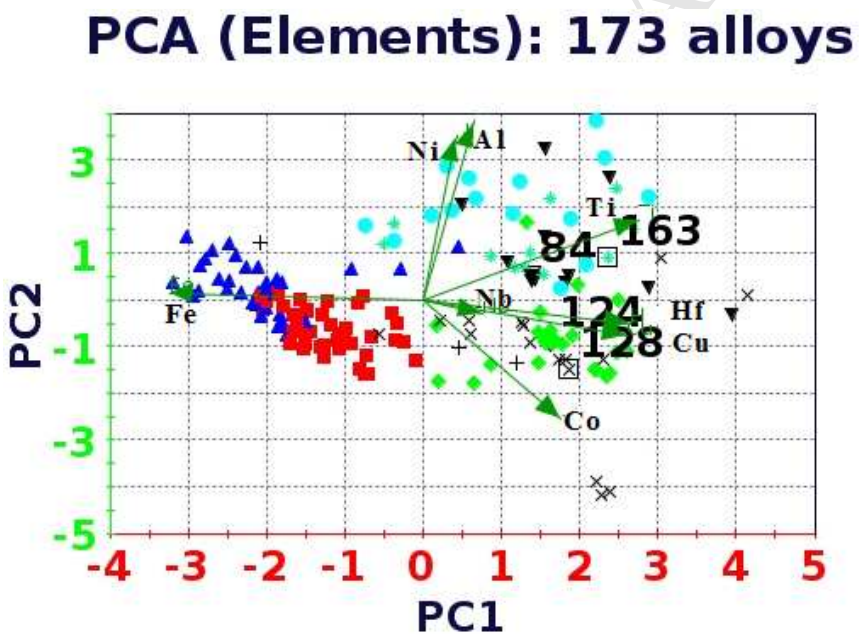

Fig. 19.

Orientation of various elements in the PC space

From Figure 19, one can observe that, Cu, Hf, Nb, and Fe contributes more towards PC1, of which Fe has the highest contribution. Ni and Al contribute more on PC2. Ti and Co has similar effect on both PC1 and PC2. Length and orientation of arrow are similar for Cu and Hf. Hence, Cu and Hf may affect the properties of alloy in the same manner. Similarly, length and orientation of arrows corresponding to Ni and Al suggests that these elements will affect the properties in the same way. One can observe that the marked alloys are clustered in a very small region while inferior alloys cover a majority of the PC space. Hence, if a certain alloy composition is near these top alloys in the PC space, then they can be given a chance over others during the selection of alloys for experimental validation.

Niobium has the lowest contribution towards PC1 while it is almost orthogonal to PC2. Hence, if we want to remove an element for rare-earth addition, we can reject Nb and manufacture a few alloys without it.

Thereafter, we used the dataset of 40 alloys selected by MCDM and performed PCA on it. This was followed by cluster analysis on the dataset by K-means clustering (Kaufman approach) method. Based on D-B index, the data set was divided into 5 clusters. Alloys belonging to different clusters are denoted by different symbols. In Figure 20, one can see that the orientation of the arrows has been altered. This is expected as these alloys were selected by MCDM, and hence this reduced set will have different variance. A few alloys have been marked in Figure 19 and 20. It can be observed that superior alloys are clustered together as alloys near these marked alloys were candidates that were part of the next set of alloys with superior properties. Hence, this method can be used for screening of the alloys prior to manufacture.

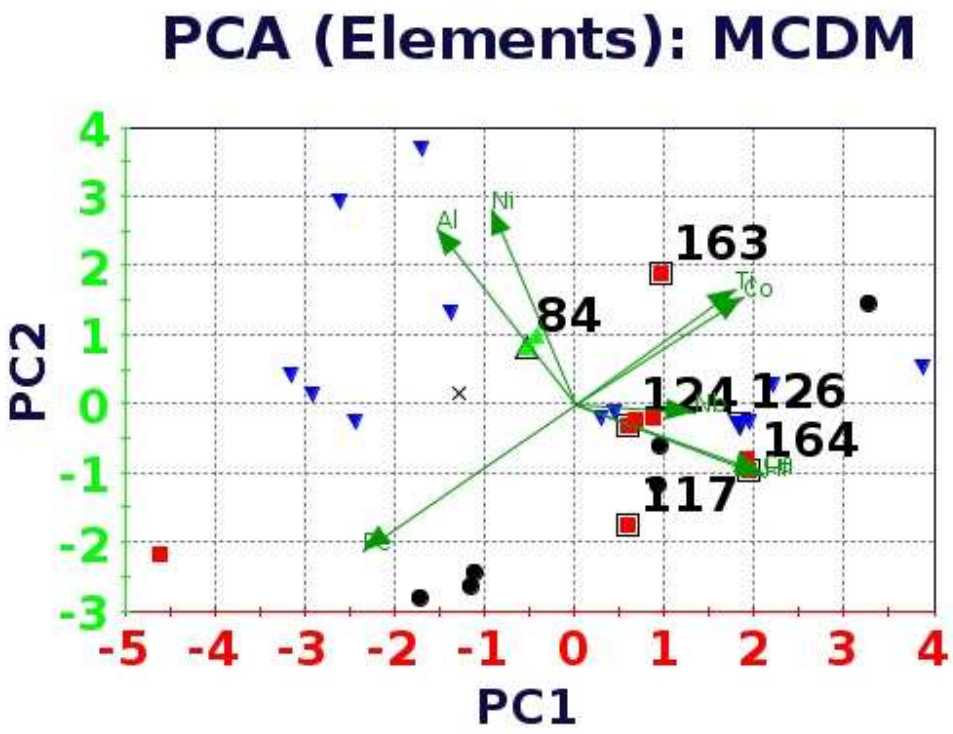

Fig. 20.

Orientation of various elements in the PC space

In this set too, arrows corresponding to Cu and Hf overlap each other, which confirms our previous findings. Arrows corresponding to Ni and Al are oriented together as observed before. Nb is almost orthogonal to PC2 and, hence, has minimal effect on it. Nb is collinear to PC1, but length of arrow is smallest for Nb along PC1. His means that Nb will have least contribution. Therefore, one can think of removing Nb from the next set of alloys and have it substituted with a rare-earth element. One peculiar finding is that Co and Ti are oriented together. This needs further investigation.

5. Discussion

In this work, we focused on ways to explore an optimum set of combinations of chemical concentrations for a single heat treatment protocol. Readers are advised to refer to the following work for better understanding of the experimental setup and detailed analysis [29, 30]. Figures 2, 3 and 4 show the scatter plots among magnetic energy density, magnetic coercivity, and magnetic remanence. Top ten alloys are marked in these figures. In these figures as well as Table 2, alloys have been ranked on the basis of $(BH)_{max}$ values. At present, the best alloy is alloy number 124. From Figures 2, 3 and 4 one can observe that the Pareto-optimized alloys (modeFRONTIER and IOSO) dominate the initial 80 candidate alloys randomly predicted by Sobol's algorithm. One can observe from the figures that we were able to improve upon Hc without compromising on B_r.

In SVR, only Nickel showed some weak/mixed response for $(BH)_{max}$. Hence, there is scope for improvement in the accuracy of the response surface algorithm. Copper was found to show a direct correlation with H_c and B_r. In this case, response surface predictions are at par with the literature. Hafnium shows positive correlation with H_c and B_r, which is promising, but needs further evaluation.

PC analysis proved to be helpful in reducing the dimensionality of the data set for visualization. PC analysis points towards a correlation between elements Cu-Hf and Ni-Al. Ni-Al rich phase is known in AlNiCo alloys and its effect on magnetic properties is supported by data from the literature. Hf has been rarely used in AlNiCo alloys and hence its similarity with Cu can be exploited to improve the magnetic properties. Hf enhances high temperature properties, hence the new magnets are supposed to have superior magnetic properties at elevated temperatures.

From Figure 19 and 20, one can see that Nb has lowest contribution on PC1, although it is collinear to it. Niobium is almost orthogonal to PC2 and hence, it will have least contribution on it. This suggests that if one needs to exclude an element from further analysis, one can think of excluding Nb and manufacture a few samples without it. These findings are quite helpful in development of knowledge base for design of new materials. At the same time, it has the potential to save time and money otherwise invested in random experimentation. PC analysis can be used as a tool to screen alloys predicted by various optimizers prior to manufacture. Alloys that are near to the previous best alloys in the PC space can be preferred for manufacture over the others for improved results.

At present, *ab-initio* based calculations, as well as Calphad approach [37], are effective for limited systems (alloys having maximum 3-4 elements), and cannot handle eight elements [37]. Use of statistical tools will be helpful in determining the most influential alloying elements. This will be helpful in theoretical validation of the above findings. Additionally, one can work on finding the most stable phases needed for enhanced performance of these alloys by focusing on the most influential elements.

6. Conclusions

Details of a new methodology for accelerated development of new permanent magnetic alloys using multi-objective optimization algorithms, meta-modeling and data mining algorithms with periodic experimental verification has been presented. The example magnetic alloy family was an AlNiCo type of alloy having eight alloying elements. We focused on finding optimal concentrations of each of the alloying elements that will result in the maximum possible (in a Pareto optimum sense) magnetic energy density, magnetic coercivity and magnetic remanence. Our design optimization approach has

the potential to overcome initial flaws that cannot be ignored in design/development of new alloys. It was demonstrated that this alloy design methodology was able to successfully and rapidly recover from the initial flaws resulting from random experimentation, which would have been impossible when using standard alloy design methods. The resulting Pareto-optimized alloy compositions rival macroscopic magnetic properties of commercial AlNiCo alloys, but have different chemical concentrations, thus, suggesting that optimization algorithms are capable of exploring yet unexplored domains of the design space. Sensitivity analysis also revealed that certain alloying elements have negligible influence on magnetic properties of the alloy and could be replaced by some of the affordable and readily available rare-earth elements. The accuracy and robustness of the entire computational effort can be further improved by developing response surfaces that maintain high accuracy even outside the available experimental data set. The presented multi-objective optimization, meta-modeling and data mining algorithms with periodic experimental verification applied to material systems under well-defined limitations of composition (used elements as well as concentration ranges) and processing steps, represent the design optimization procedure that could be successful also for other systems that are characterized by other coercivity mechanisms based on other microstructures. Therefore, optimization of alloy composition has to be accompanied by optimization of processing which means incorporating additional design variables defining temperature *versus* time protocols and applied magnetic field *versus* time protocols.

Acknowledgements

This work was partially funded by the US Air Force Office of Scientific Research under grant FA9550-12-1-0440 monitored by Dr. Ali Sayir. The lead author is also thankful to

University Graduate School, Florida International University for providing him funding in the form of Dissertation Year Fellowship. Authors are grateful for the highly competent and constructive reviewers' comments. The views and conclusions contained herein are those of the authors and should not be interpreted as necessarily representing the official policies or endorsements, either expressed or implied, of the US Air Force Office of Scientific Research or the U.S. Government. The U.S. Government is authorized to reproduce and distribute reprints for government purposes notwithstanding any copyright notation thereon.

References

[1] P. Mcguiness, O. Akdogan, A. Asali, S. Bance, F. Bittner, J.M.D. Coey, N.M. Dempsey, J. Fidler, D. Givord, O. Gutfleisch, M. Katter, D. Le Roy, S. Sanvito, T. Schrefl, L. Schultz, C. Schwöbl, M. Soderžnik, S. Šturm, P. Tozman, K. Űstűner, M. Venkatesan, T.G. Woodcock, K. Žagar, S. Kobe, Replacement and Original Magnet Engineering Options (ROMEOs): A European Seventh Framework Project to Develop Advanced Permanent Magnets Without, or with Reduced Use of, Critical Raw Materials. JOM, 67, (2015) 1306–1317.

[2] B.D. Cullity, C. Graham, Chapter 14. Hard magnetic materials. In: Introduction to Magnetic Materials, Second Edition, Wiley-IEEE Press, New York (2009) 477-504.

[3] F. Ronning, S. Bader, Rare earth replacement magnets. Journal of Physics: Condensed Matter, 26, (2014) 1–3.

[4] M.J. Kramer, R.W. McCallum, I.A. Anderson, S. Constantinides, Prospects for non-rare earth permanent magnets for traction motors and generators. JOM, 64, (2012) 752–763.

[5] D.J. Sellmyer, B. Balamurugan, W.Y. Zhang, B. Das, R. Skomski, P. Kharel, Y. Liu, Advances in rare-earth-free permanent magnets. The 8th Pacific Rim International Congress on Advanced Materials and Processing (PRICM8), Waikoloa, Hawaii (4-9 August 2013).

[6] L. Zhou, M. Miller, P. Lu, L. Ke, R. Skomski, H. Dillon, Q. Xing, A. Palasyuk, M. McCartney, D. Smith, S. Constantinides, R. McCallum, I. Anderson, V. Antropov, M. Kramer, Architecture and magnetism of AlNiCo. Acta Materialia, 74, (2014) 224–233.

[7] K. Rajan (eds), Materials informatics: An introduction. Informatics for Materials Science and Engineering: Data-Driven Discovery for Accelerated Experimentation and Application, 1st edition, Elsevier, (2013) 1–120.

[8] M.F. Horstemeyer, Integrated Computational Materials Engineering (ICME) for Metals: Using Multiscale Modeling to Invigorate Engineering Design with Science. TMS - The Minerals, Metals and Materials Society, John Willey and Sons, Inc.), Hoboken, New Jersey (2012).

[9] I.N. Egorov-Yegorov, G.S. Dulikravich, Chemical composition design of superalloys for maximum stress, temperature, and time-to-rupture using self-adapting response surface optimization. Materials and Manufacturing Processes, 20 (2005) 569–590.

[10] R. Jha, G.S. Dulikravich, F. Pettersson, H. Saxen, N. Chakraborti, A combined experimental-computational approach to design optimization of high temperature alloys. In: ASME Symposium on Elevated Temperature Application of Materials for Fossil, Nuclear, and Petrochemical Industries, ASME, Seattle, WA (March 25-27, 2014).

[11] R. Jha, G.S. Dulikravich, M. Fan, J. Shwartz, C.C. Koch, I.N. Egorov, C.A. Poloni, A combined computational-experimental approach to design of high-intensity permanent magnetic alloys. CONEM2014, Uberlandia, Brazil (August 10-15, 2014).

[12] R. Jha, F. Pettersson, G.S. Dulikravich, H. Saxen, N. Chakraborti, Evolutionary design of nickel-based superalloys using data-driven genetic algorithms and related strategies. Materials and Manufacturing Processes, 30, 4, (2015) 488–510.

[13] R. Jha, G.S. Dulikravich, M.J. Colaco, Design and optimization of magnetic alloys and nickel-based superalloys for high temperatures applications, COBEM-2015, paper 1284, Rio de Janeiro, Brazil, (6-11 December, 2015).

[14] R. Rettig, N.C. Ritter, H.E. Helmer, S. Neumeier, R.F. Singer, Single-crystal nickel-based superalloys developed by numerical multi-criteria optimization techniques: design based on thermodynamic calculations and experimental validation. Modelling and Simulation in Materials Science and Engineering, 23, 3, (2015) 035004.

[15] G.S. Dulikravich, I.N. Egorov, Inverse Design of Alloys' Chemistry for Specified Thermo-Mechanical Properties by Using Multi-Objective Optimization, Chapter 8 in Computational Methods for Applied Inverse Problems (eds: Y.F. Wang, A.G. Yagola, C.C. Yang), Inverse and Ill-Posed Problems Series 56, Walter De Gruyter and Higher Education Press, China, ISBN: 978-3-11-025905-6, (12 September 2012) 197-219.

[16] Thermocalc: http://www.thermocalc.com/solutions/by-application/alloy-development/, accessed on 3/1/2015 (2015).

[17] I. Toda-Caraballo, P.E.J. Rivera-Diaz-Del-Castillo, Modelling and design of magnesium and high entropy alloys through combining statistical and physical models. JOM, 67, 1 (2015) 108–117.

[18] N. Settouti, H. Aourag, A study of the physical and mechanical properties of lutetium compared with those of transition metals: A data mining approach. JOM, 67, 1 (2015) 87–93.

[19] T. Mueller, A. Kusne, R. Ramprasad, Machine learning in materials science: Recent progress and emerging applications. Reviews in Computational Chemistry, 29 (2016).

[20] A.G. Kusne, T. Gao, A. Mehta, L. Ke, M.C. Nguyen, K.M. Ho, V. Antropov, C.Z. Wang, M.J. Kramer, C. Long, I. Takeuchi, On-the-fly machine-learning for high-throughput experiments; search for rare-earth-free permanent magnets, Scientific Reports 4 published online (15 September 2014) article no. 6367, doi:10.1038/srep06367.

[21] H. Dilon, Effects of heat treatment and processing modifications on microstructure in AlNiCo-8H permanent magnetic alloys for high temperature applications. Graduate thesis and dissertations, Iowa State University, http:/lib.dr.iastate.edu/etd/13867 (2014), paper 13867.

[22] Q. Xing, M.K. Miller, L. Zhou, H.M. Dillon, R.W. McCallum, I. Anderson, S. Constantinides, M.J. Kramer, Phase and elemental distributions in AlNiCo magnetic materials. IEEE Transactions on Magnetics, 49, 7, (2013) 3314–3317.

[23] R. Jha, G.S. Dulikravich, M.J. Colaco, M. Fan, J. Schwartz, C.C. Koch, Magnetic alloys design using multi-objective optimization, to appear in Advanced Structured Materials series (eds.: Oechsner, A., da Silva, L.M., Altenbach, H.), Springer, Germany (2016).

[24] R. McCallum, L. Lewis, R. Skomski, A. Kramer, I.A. Anderson, Practical aspects of modern and future permanent magnets. Annual Review of Materials Research, 44, 1, (2014) 451–477.

[25] N. Makino, Y. Kimura, Techniques to achieve texture in permanent magnet alloy systems, Journal of Applied Physics, 36(3), (1965) 1185–1190.

[26] S. Pramanik, V. Rao, O.N. Mohanity, Effect of niobium on the directional solidification and properties of AlNiCo alloys, Journal of Materials Science, 28, (1993) 1237-1244.

[27] I.M. Sobol, Distribution of points in a cube and approximate evaluation of integrals. U.S.S.R. Comput. Maths. Math. Phys, 7, (1967) 86-112.

[28] Factsage, http://www.factsage.com/, accessed on 3/1/2015 (2015).

[29] M. Fan, Y. Liu, R. Jha, G. S. Dulikravich, J. Schwartz and C. Koch, Microscopic Characterization of Cu-Ni-rich Bridges in AlNiCo Alloys, 13th Joint MMM-Intermag Conference, January 11-15 (2016).

[30] M. Fan, Y. Liu, R. Jha, G. S. Dulikravich, J. Schwartz and C. Koch, Effect of Cu-Ni-rich Bridges on the Microstructure and Magnetic Properties of AlNiCo Alloys, IEEE Transactions on Magnetics, TMAG-16-01-0076, (under review).

[31] ESTECO: modeFRONTIER, http://www.esteco.com/modefrontier, accessed on 3/1/2015 (2015).

[32] G.S. Dulikravich, M.J. Colaco, Hybrid optimization algorithms and hybrid response surfaces. In: Advances in Evolutionary and Deterministic Methods for Design, Optimization and Control in Engineering and Sciences, (D. Greiner; B. Galvn; J. Periaux; N. Gauger; K. Giannakoglou; G. Winter, eds.), Chapter 2, Springer Verlag, Heidelberg (2015) 19-47.

[33] K. Deb, Multi-objective optimization using evolutionary algorithms. John Wiley and Sons, Chichester, UK (2001).

[34] F. Pettersson, N. Chakraborti, H. Saxen, A genetic algorithms based multi-objective neural net applied to noisy blast furnace data. Applied Soft Computing, 7, 1, (2007) 387–397.

[35] B.K. Giri, J. Hakanen, K.Miettinen, N. Chakraborti, Genetic programming through bi-objective genetic algorithms with a study of a simulated moving bed process involving multiple objectives. Applied Soft Computing Journal, 13, 5, (2013) 2613–2623.

[36] IBMSPSS: IBM corp. released 2013. IBM spss statistics for windows, version 22.0. armonk, ny: Ibm corp., http://www-01.ibm.com/software/analytics/spss/, accessed on 3/1/2015 (2015).

[37] P.J. Spencer, A brief history of CALPHAD. Calphad, 32, 1, (2008) 1–8.